[15] M. Cheffena and T. Ekman, "Dynamic model of signal fading due to swaying vegetation," *EURASIP J. Wireless Commun. Networking. Special Issue on Advances in Propagation Modelling for Wireless Systems*, vol. 2009, no. Article ID 306876, doi:10.1155/2009/306876, p. 11, 2009.
[16] M. Cheffena and T. Ekman, "Theoretical multipath channel model during rain for BFWA employed in dense urban areas," presented at the ICSPCS, Gold Coast, Australia, Dec. 15–17, 2008.
[17] J. C. Liberti and T. S. Rappaport, "A geometrically based model for line-of-sight multipath radio channels," in *Proc. IEEE Veh. Tech. Conf.*, 1996, pp. 844–848.
[18] P. Soma, L. Cheun, S. Sun, and M. Y. W. Chia, "Propagation measurements and modelling of LMDS radio channel in Singapore," *IEEE Trans. Veh. Techn.*, vol. 52, no. 3, pp. 595–606, May 2003.
[19] P. B. Papazia, G. A. Hufford, and R. J. Achatz, "Study of the local multipoint distribution service radio channel," *IEEE Trans. Broad.*, vol. 43, pp. 175–184, 1997.
[20] H. Xu, T. S. Rappaport, R. J. Boyle, and J. H. Schaffner, "Measurements and models for 38 GHz point-to-multipoint radiowave propagation," *IEEE J. Areas Commun.*, vol. 18, no. 3, pp. 310–321, Mar. 2000.
[21] P. Hou, J. Zhuang, and G. Zhang, "A rain fading simulation model for broadband wireless access channels in millimeter wavebands," presented at the 51st IEEE VTC Spring, Tokyo, Japan, 2000.
[22] A. D. Panagopoulos, K. P. Liolis, and P. G. Cottis, "Rician K-factor distribution in broadband fixed wireless access channels under rain fades," *IEEE Commun. Lett.*, vol. 11, pp. 301–303, Apr. 2007.
[23] I. J. Dilworth and B. L. Ebraly, "Propagation effects due to foliage and building scatter at millimeter wavelengths," in *Proc. Inst. Elect. Eng. Antennas Propag. Conf.*, Apr. 4–7, 1995, pp. 51–53.

Planar Printed Strip Monopole With a Closely-Coupled Parasitic Shorted Strip for Eight-Band LTE/GSM/UMTS Mobile Phone

Fang-Hsien Chu and Kin-Lu Wong

***Abstract*—A planar printed antenna comprising a driven strip monopole and a parasitic shorted strip, both of comparable length and closely coupled to each other, suitable for eight-band LTE/GSM/UMTS operation in the mobile phone is presented. The proposed antenna is mainly configured along the boundary of the no-ground portion on the system circuit board of the mobile phone to achieve a simple and compact structure. Also, the edge of the no-ground portion facing the system ground plane on the circuit board is not necessarily a straight line, leading to more degrees of freedom in allocating the required no-ground portion on the circuit board for printing the antenna. The driven strip monopole and the parasitic shorted strip both contribute their lowest and higher-order resonant modes to form two wide operating bands centered at about 830 and 2200 MHz to respectively cover the LTE700/GSM850/900 operation (698–960 MHz) and GSM1800/ 1900/UMTS/LTE2300/2500 operation (1710–2690 MHz).**

***Index Terms*—Handset antennas, internal handset antennas, mobile antennas, printed monopoles, small antennas.**

I. Introduction

Planar strip monopole is suitable to be printed on one surface of the system circuit board of the mobile phone, making it easy to fabricate at low cost and find applications in the slim or thin-profile mobile phone [1]–[10] for its negligible antenna thickness above the system circuit board. Some promising planar strip monopoles for penta-band WWAN (wireless wide area network) operation covering the GSM850 (824–894 MHz), GSM900 (880–960 MHz), GSM1800 (1710–1880 MHz), GSM1900 (1850–1990 MHz) and UMTS (1920–2170 MHz) bands have been reported in the published papers [11]–[14]. To achieve small size yet wideband or multiband operation, the techniques of embedding a chip inductor [11], [12] or using an internal printed distributed inductor [13] in the strip monopole have been demonstrated. The design using a printed distributed inductor to replace the embedded chip inductor facilitates the fabrication of the antenna on the system circuit board. The use of an external matching network is also helpful in achieving improved impedance matching for frequencies over the desired lower band (824–960 MHz) and upper band (1710–2170 MHz) for penta-band WWAN operation [11], although the external matching networks may cause some undesired loss in the input power of the antenna. In these designs, however, the obtained bandwidth cannot cover the recently introduced LTE (long term evolution) operation [15]–[17] in the 700 MHz band (698–787 MHz), 2300 MHz band (2305–2400 MHz) and 2500 MHz band (2500–2690 MHz). The LTE operation is expected to provide better mobile broadband and multimedia services than the existing GSM and UMTS communication systems and will become attractive for the mobile users. Hence, the mobile phone capable of eight-band operation including the LTE700/2300/2500, GSM850/900/1800/1900, and UMTS bands will be demanded on the market in the very near future.

In this communication we present a novel planar printed strip monopole to cover the desired eight-band LTE/GSM/UMTS operation. The proposed planar monopole has a simple structure which comprises a driven strip monopole and a parasitic shorted strip, both of comparable length and closely coupled to each other. The parasitic shorted strip used in the proposed design is different from the traditional ones that have been applied in the internal mobile device antennas [18]–[21] for bandwidth enhancement, in which the parasitic strip is usually of a much shorter length than the driven element; furthermore, only part of the parasitic strip is gap-coupled to the driven element or vice versa. In the proposed design, both the driven strip monopole and the parasitic shorted strip whose length is slightly longer than that of the driven strip monopole contribute their lowest (0.25λ) resonant modes to form a wide operating band centered at about 830 MHz for the antenna's lower band to cover the frequency range of 698–960 MHz. A wide operating band centered at about 2200 MHz for the frequency range of 1710–2690 MHz is also obtained, which is formed by the higher-order resonant modes contributed by both the driven and parasitic shorted strips. That is, the proposed planar monopole can provide two wide lower and upper bands to respectively cover the LTE700/GSM850/900 and GSM1800/1900/UMTS/ LTE2300/2500 operation. In addition, the simple structure of the proposed antenna allows it to easily follow along the boundary of the no-ground portion on the system circuit board of the mobile phone such that the antenna can be implemented with a small printed area. The proposed design is also promising to be implemented in the no-ground portion with a non-straight edge facing the main ground plane on the system circuit board. This can lead to more degrees of freedom in allocating the required no-ground portion for printing the antenna on the system circuit board. Detailed operating principle of the proposed antenna is described in the communication, and the proposed antenna is fabricated and studied.

II. Proposed Antenna

Fig. 1 shows the geometry of the proposed antenna having a simple uniplanar structure and comprising only two elements: a driven strip

Manuscript received October 31, 2009; revised January 25, 2010; accepted April 06, 2010. Date of publication July 01, 2010; date of current version October 06, 2010.

The authors are with the Department of Electrical Engineering, National Sun Yat-sen University, Kaohsiung 80424, Taiwan (e-mail: wongkl@mail.nsysu.edu.tw; http://antenna.ee.nsysu.edu.tw).

Color versions of one or more of the figures in this communication are available online at http://ieeexplore.ieee.org.

Digital Object Identifier 10.1109/TAP.2010.2055807

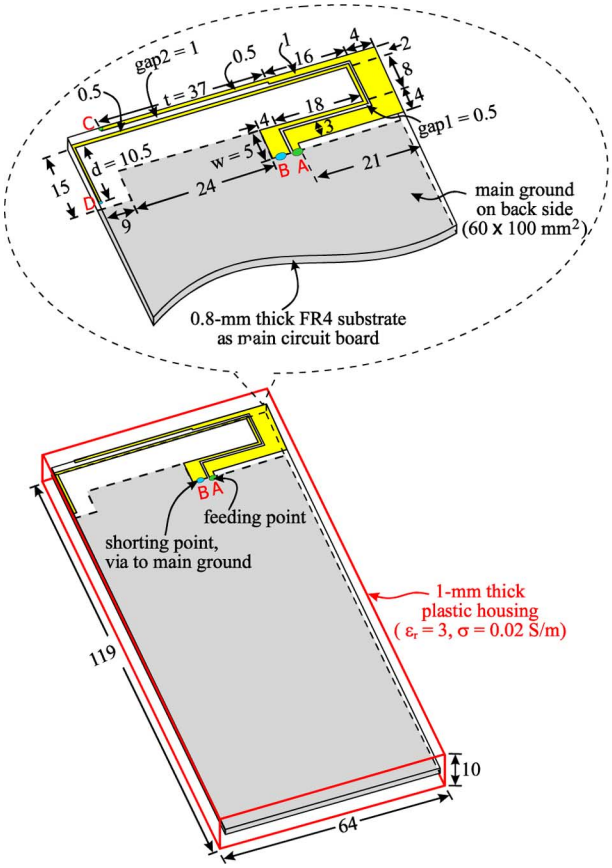

Fig. 1. Geometry of the proposed antenna for eight-band LTE/GSM/UMTS operation in the mobile phone.

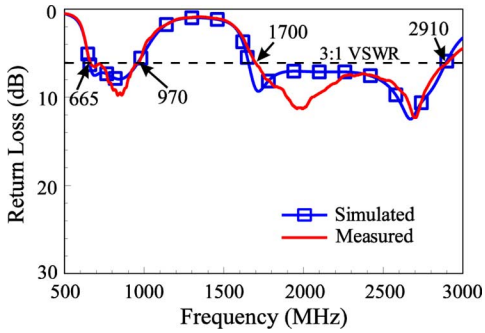

Fig. 2. Measured and simulated return loss for the proposed antenna.

monopole (section AC) and a closely-coupled parasitic shorted strip (section BD). A no-ground portion with a non-straight edge facing the system ground plane printed on the system circuit board is allocated to accommodate the proposed antenna. In the study, a 0.8-mm thick FR4 substrate of length 115 mm and width 60 mm is used as the system circuit board, which is further enclosed by a plastic housing fabricated using the plastic plates of thickness 1 mm, relative permittivity 3.0, and conductivity 0.02 S/m as the mobile phone housing. The no-ground portion has a size of about 780 mm^2 (15×60 mm^2 less the extended ground of size 5×24 mm^2 in the system ground plane). The driven strip monopole and parasitic shorted strip of the proposed antenna generally follow along the boundary of the no-ground portion to achieve a compact structure. The front end (point A) of the driven strip monopole is the feeding point of the antenna, while the front end (point B) of the parasitic shorted strip is short-circuited to the top edge of the system ground plane through a via-hole in the system circuit board.

In-between the driven strip monopole and parasitic shorted strip, there are a first coupling gap (gap1) of 0.5 mm in the front section and a second coupling gap (gap2) of 1.0 mm in the remaining section of length 37 mm (t). The use of two coupling gaps leads to more degrees of freedom in adjusting the capacitive coupling between the two strips, which makes it easy to achieve good impedance matching (better than 3:1 VSWR or 6-dB return loss widely used as the mobile phone antenna specification in the practical applications) for frequencies over the desired operating bands. The lengths of the driven strip monopole and parasitic shorted strips are both close to a quarter-wavelength (about 93 mm) at 800 MHz, but are of slightly different lengths. The two strips are expected to contribute their lowest resonant modes, with one at frequencies lower than about 800 MHz and the other one at frequencies higher than about 800 MHz; the two resonant modes can be incorporated into a wide lower band for the proposed antenna to cover the desired frequency range of 698–960 MHz.

In addition, the parasitic shorted strip can contribute its two higher-order resonant modes to occur at about 1700 and 2700 MHz, which can incorporate the higher-order resonant modes of the driven strip monopole occurred at about 2200 and 2600 MHz to form a very wide upper band (bandwidth larger than 1 GHz) to cover the desired frequency range of 1710–2690 MHz. Details of the excited resonant modes will be discussed with the aid of Fig. 3 in the next section. Further, note that the extended ground (size 5×24 mm^2) at the top edge of the system ground plane can be used to accommodate the associated nearby electronic elements such that some valuable board space can be reclaimed for use, which is attractive for practical applications.

III. Results and Discussion

The proposed antenna with dimensions given in Fig. 1 was fabricated and tested. Results of the measured and simulated return loss for the fabricated prototype are shown in Fig. 2. The simulated results in this study are obtained using Ansoft HFSS version 11.2 [22]. The measured data generally agree with the simulated results. Two wide operating bands are seen to be excited. The lower band, based on the definition of 3:1 VSWR or 6-dB return loss, shows a wide bandwidth of 305 MHz (665–970 MHz) which allows the antenna to cover the LTE700/GSM850/900 operation. The upper band shows an even wider bandwidth of 1210 MHz (1700–2910 MHz), which covers the GSM1800/1900/UMTS/LTE2300/2500 operation. Hence, with the obtained wide lower and upper bands, eight-band LTE/GSM/UMTS operation is achieved for the proposed antenna.

To analyze the operating principle of the proposed antenna, Fig. 3 shows the comparison of the simulated return loss and input impedance of the proposed antenna and the reference antenna (the corresponding antenna without the parasitic shorted strip). Notice that the driven strip monopole (section AC) in the two antennas tested in the figure is with the same dimensions. In Fig. 3(a), for the reference antenna, the lower band is centered at about 950 MHz and formed by one resonant mode only. The bandwidth of this lower band cannot cover the desired frequency range of 698–960 MHz. Similarly, the upper band of the reference antenna is formed by one resonant mode at about 2200 MHz, whose bandwidth is far from covering the desired frequency range of 1710–2690 MHz. When the parasitic shorted strip is added (the proposed antenna), an additional resonant mode at about 700 MHz (denoted as mode p1 in the figure) is generated; this can be seen more clearly from the input impedance results shown in Fig. 3(b). This new resonant mode incorporates the original one (mode d1 in the figure) contributed by the driven strip monopole to form a wide lower band for the 698–960 MHz operation. Also note that mode d1 shifted down with the adding of the parasitic shorted strip is mainly because the length of

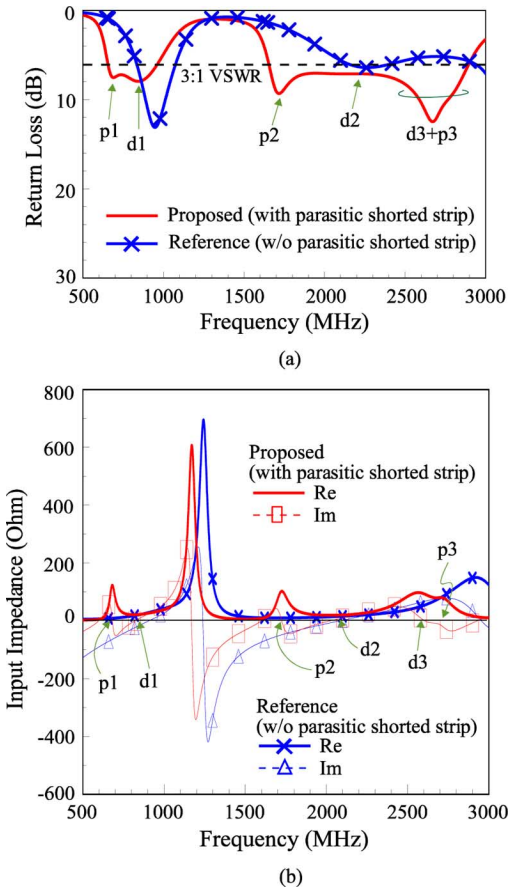

Fig. 3. Comparison of the simulated (a) return loss and (b) input impedance of the proposed antenna and the reference antenna (without the parasitic shorted strip).

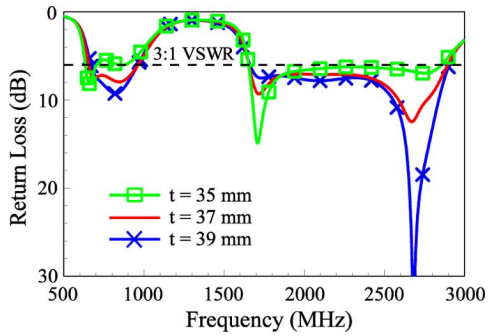

Fig. 4. Simulated return loss as a function of the end-section length t of the driven strip monopole; other dimensions are the same as given in Fig. 1.

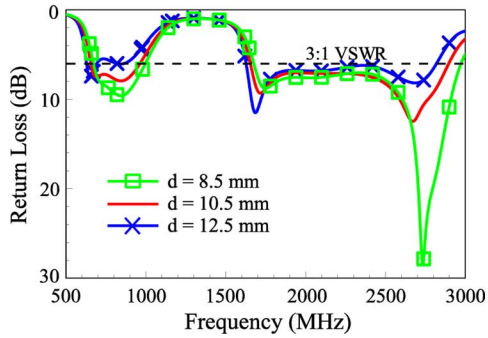

Fig. 5. Simulated return loss as a function of the end-section length d of the parasitic shorted strip; other dimensions are the same as given in Fig. 1.

the parasitic shorted strip is slightly longer than that of the driven strip monopole and there is also strong coupling between the two coupled strips.

Two higher-order resonant modes of the parasitic shorted strip are also excited at about 1700 and 2700 MHz (mode p2 and p3 in the figure) with good impedance matching [also see the input impedance results in Fig. 3(b)]. There are also two higher-order resonant modes at about 2200 and 2600 MHz (mode d2 and d3 in the figure) contributed by the driven strip monopole. Note that the mode at about 2600 MHz is related to the one at about 2900 MHz for the case of no parasitic shorted strip; when the parasitic shorted strip is added, the mode at about 2900 MHz is shifted to lower frequencies at about 2600 MHz. A wide upper band is then formed by these higher-order resonant modes contributed by the parasitic shorted strip and the driven strip monopole to cover the 1710–2690 MHz band operation.

A parametric study of the proposed antenna is also conducted. Fig. 4 shows the simulated return loss as a function of the end-section length t of the driven strip monopole. Large effects on both the antenna's lower and upper bands are observed. With the decreased length t, the resonant mode contributed by the driven strip monopole is greatly affected and is shifted to higher frequencies (see the second resonant mode in the lower band). In addition, the decreased length t also leads to degraded impedance matching for the resonant modes contributed by the parasitic shorted strip. This is largely because the decreased length t decreases the coupling-gap length of gap2, which affects the capacitive coupling between the driven strip monopole and the parasitic shorted strip and hence results in degraded impedance matching for the resonant modes excited through the capacitive coupling.

Fig. 5 shows the effects of the end-section length d of the parasitic shorted strip. Results of the simulated return loss for the length d varied from 8.5 to 12.5 mm are shown. Large effects on both the antenna's lower and upper bands are also seen. In addition, it is noted that the central or resonant frequencies of the resonant modes contributed by the parasitic shorted strip are varied (see the first mode at about 700 MHz in the lower band and the two modes at the lower edge and upper edge of the upper band). This further confirms the contribution of the parasitic shorted strip in the excited resonant modes for the proposed antenna.

Fig. 6 shows the effects of the width w of the extended ground. Results of the simulated return loss for the width w varied from 3 to 7 mm are presented. Small variations in the obtained bandwidth of the upper band are seen. However, when the width w is increased, that is, the extended ground is extended further into the no-ground portion, the obtained bandwidth of the lower band is decreased. For covering the desired operating band of 698–960 MHz, the width w is selected to be 5 mm here.

The measured three-dimensional (3-D) total-power radiation patterns for the proposed antenna are plotted in Fig. 7. The antenna is tested in a far-field anechoic chamber [TRC (Training Research Co.) measurement system]. Measured results for frequencies at 740, 925, 1795, 2045 and 2400 MHz are shown. The radiation patterns for frequencies in the lower band generally show dipole-like patterns, and omnidirectional radiation in the azimuthal plane ($x-y$ plane) is observed. On the other hand, more variations and nulls in the radiation patterns are seen for frequencies in the upper band. Note that the radiation patterns of the internal mobile phone antenna are generally dependent on the system ground plane of the mobile phone which is also an efficient radiator [23]–[25], especially for frequencies in the lower band. For frequencies in the upper band, since the wavelength is comparable to the length of the system ground plane, surface current nulls are usually

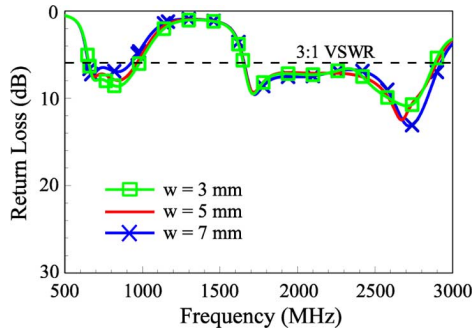

Fig. 6. Simulated return loss as a function of the width w of the extended ground; other dimensions are the same as given in Fig. 1.

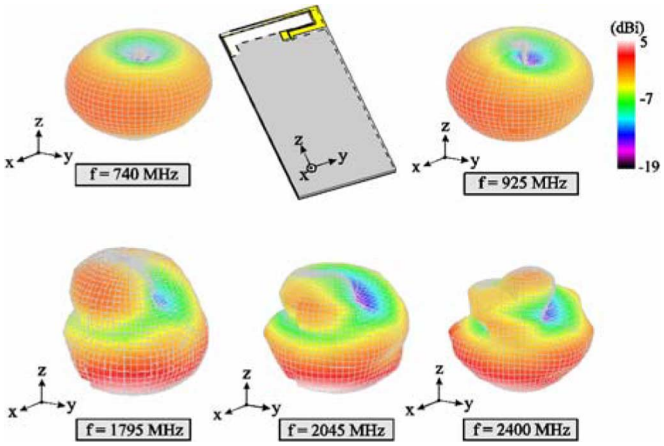

Fig. 7. Measured three-dimensional (3-D) total-power radiation patterns for the proposed antenna.

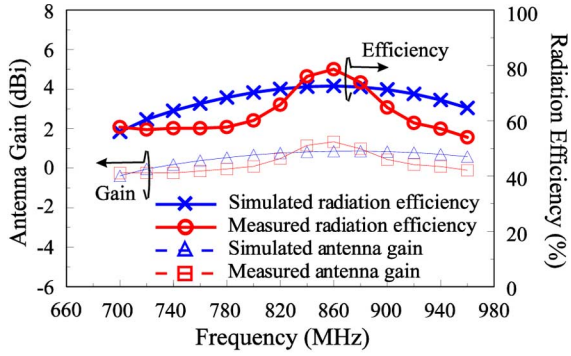

(a)

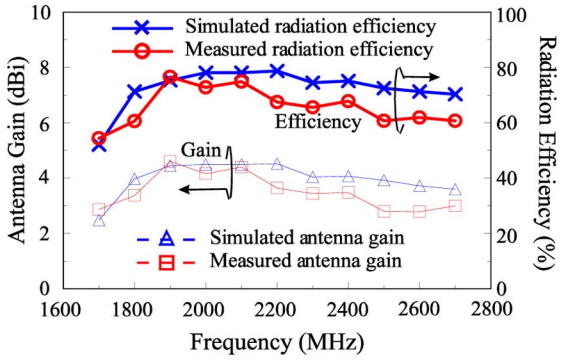

(b)

Fig. 8. Measured and simulated antenna gain and radiation efficiency for the proposed antenna. (a) The lower band (698–960 MHz). (b) The upper band (1710–2690 MHz).

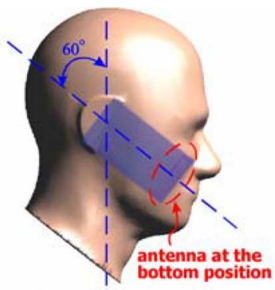

Frequency (MHz)	740	859	925	1795	1920	2045	2350	2595
1-g SAR (W/kg)	1.00	0.94	0.92	0.41	0.48	0.50	0.40	0.33
Return loss (dB)	15.5	7.4	6.2	6.7	9.5	8.5	6.1	7.7

Fig. 9. SAR simulation model (SEMCAD [26]) and the simulated SAR values for 1-g head tissue for the proposed antenna. The return loss given in the table shows the impedance matching level at the testing frequency.

excited in the system ground plane which leads to the nulls or large variations observed in the radiation patterns at higher frequencies.

Fig. 8 presents the measured and simulated antenna gain and radiation efficiency for the proposed antenna. The measured data generally agree with the simulated results. Over the lower band (698–960 MHz) and upper band (1710–2690 MHz) respectively shown in Fig. 8(a) and (b), the measured antenna gain is about -0.4–1.1 dBi and 2.7–4.4 dBi. The measured radiation efficiency is respectively about 53–76% and 52–75% over the lower and upper bands. The radiation efficiency for all the frequencies in the lower and upper bands is all better than 50% for the proposed antenna, which generally is acceptable for practical applications in the modern mobile phones.

The SAR (specific absorption rate [26]) results are studied in Fig. 9. The SAR simulation model (SEMCAD [27]) shown in the figure is applied. Note that the mobile phone in the study is with the proposed antenna positioned at the bottom of system circuit board, which has been shown to be a promising arrangement for practical applications of the printed antennas with no back ground plane to achieve decreased SAR values [7], [8], [28], [29]. The simulated SAR values for 1-g head tissue are listed in the table in the figure. The return loss given in the table shows the impedance matching level at the testing frequency. The SAR values are obtained using input power of 24 dBm for the GSM850/900 operation (859, 925 MHz) and 21 dBm for the GSM1800/1900 operation (1795, 1920 MHz), UMTS operation (2045 MHz) and LTE operation (740, 2350, 2595 MHz). The obtained SAR values are all well below the SAR limit of 1.6 W/kg [26], indicating that the proposed antenna is promising for practical mobile phone applications.

Fig. 10 shows the comparison of the simulated radiation efficiency and antenna gain of the proposed antenna with and without the plastic housing. Relatively large effects on the radiation efficiency in the lower band (698–960 MHz) than in the upper band (1710–2690 MHz) are observed. This is largely owing to the larger radiation power absorption by the plastic housing (a lossy material) for the frequencies in the lower band. The plastic housing could also cause some variations on the radiation patterns, especially in the upper band. This results in the antenna gain increase seen in some frequencies when the plastic housing is present.

Fig. 11 shows the simulated surface current distributions for the proposed antenna. From the surface current distributions, it can be seen that the parasitic shorted strip is excited at its fundamental mode at 700 MHz and its higher-order modes at 1700 and 2700 MHz. While the driven strip monopole is excited at its fundamental mode at 850 MHz

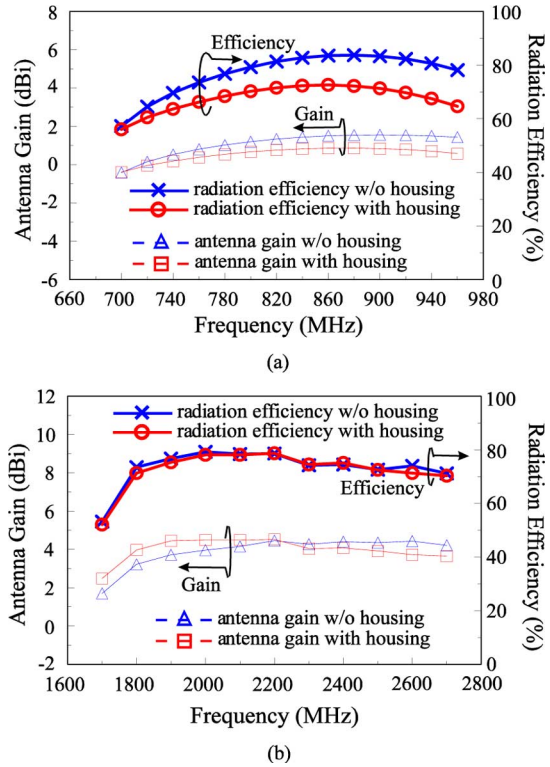

Fig. 10. Simulated antenna gain and radiation efficiency for the proposed antenna with and without the plastic housing.

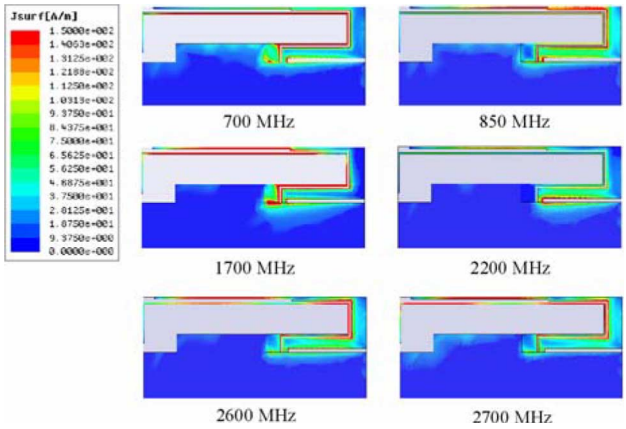

Fig. 11. Simulated surface current distributions for the proposed antenna.

and its higher-order modes at 2200 and 2600 MHz. Also note that, due to strong coupling through the coupling gap, large surface currents are excited for both the driven strip monopole and parasitic shorted strip, for example, at 2600 and 2700 MHz.

Fig. 12 shows the simulated return loss as a function of the length L of the main ground. Large effects on the lower band are observed. This behaviour is similar to those observed for the conventional internal mobile phone antennas that have been reported [23]–[25].

IV. Conclusion

A planar printed strip monopole with a closely-coupled parasitic shorted strip suitable for LTE/GSM/UMTS operation has been proposed. The antenna has been fabricated and tested. Two wide operating bands for covering the 698–960 MHz and 1710–2690 MHz bands

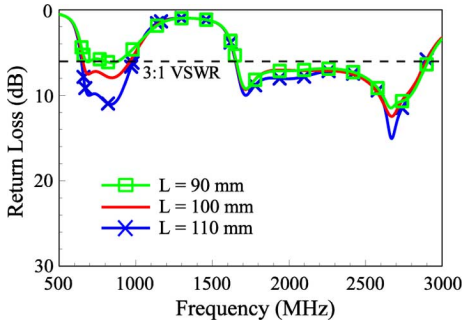

Fig. 12. Simulated return loss as a function of the length L of the main ground; other dimensions are the same as given in Fig. 1.

for the desired eight-band LTE/ GSM/UMTS operation have been obtained. Good radiation characteristics for frequencies over the operating bands have also been observed. Further, the proposed antenna can be easily printed on the small no-ground portion of about 780 mm^2 on the system circuit board of the mobile phone. The planar two-dimensional structure of the proposed antenna makes it very attractive for practical applications in the modern slim mobile phones.

References

[1] K. L. Wong, Y. C. Lin, and T. C. Tseng, "Thin internal GSM/DCS patch antenna for a portable mobile terminal," *IEEE Trans. Antennas Propag.*, vol. 54, pp. 238–242, Jan. 2006.

[2] K. L. Wong, Y. C. Lin, and B. Chen, "Internal patch antenna with a thin air-layer substrate for GSM/DCS operation in a PDA phone," *IEEE Trans. Antennas Propag.*, vol. 55, pp. 1165–1172, Apr. 2007.

[3] C. I. Lin and K. L. Wong, "Printed monopole slot antenna for internal multiband mobile phone antenna," *IEEE Trans. Antennas Propag.*, vol. 55, pp. 3690–3697, Dec. 2007.

[4] R. A. Bhatti, Y. T. Im, J. H. Choi, T. D. Manh, and S. O. Park, "Ultra-thin planar inverted-F antenna for multistandard handsets," *Microwave Opt. Technol. Lett.*, vol. 50, pp. 2894–2897, Nov. 2008.

[5] R. A. Bhatti and S. O. Park, "Octa-band internal monopole antenna for mobile phone applications," *Electron. Lett.*, vol. 44, pp. 1447–1448, Dec. 2008.

[6] H. Rhyu, J. Byun, F. J. Harackiewicz, M. J. Park, K. Jung, D. Kim, N. Kim, T. Kim, and B. Lee, "Multi-band hybrid antenna for ultra-thin mobile phone antenna," *Electron. Lett.*, vol. 45, pp. 773–774, Jul. 2009.

[7] C. H. Chang and K. L. Wong, "Printed $\lambda/8$-PIFA for penta-band WWAN operation in the mobile phone," *IEEE Trans. Antennas Propag.*, vol. 57, pp. 1373–1381, May 2009.

[8] Y. W. Chi and K. L. Wong, "Quarter-wavelength printed loop antenna with an internal printed matching circuit for GSM/DCS/PCS/UMTS operation in the mobile phone," *IEEE Trans. Antennas Propag.*, vol. 57, Sep. 2009.

[9] C. T. Lee and K. L. Wong, "Uniplanar coupled-fed printed PIFA for WWAN/WLAN operation in the mobile phone," *Microwave Opt. Technol. Lett.*, vol. 51, pp. 1250–1257, May 2009.

[10] K. L. Wong and W. Y. Chen, "Small-size printed loop antenna for penta-band thin-profile mobile phone application," *Microwave Opt. Technol. Lett.*, vol. 51, pp. 1512–1517, Jun. 2009.

[11] T. W. Kang and K. L. Wong, "Chip-inductor-embedded small-size printed strip monopole for WWAN operation in the mobile phone," *Microwave Opt. Technol. Lett.*, vol. 51, pp. 966–971, Apr. 2009.

[12] K. L. Wong and S. C. Chen, "Printed single-strip monopole using a chip inductor for penta-band WWAN operation in the mobile phone," *IEEE Trans. Antennas Propag.*, vol. 58, Jan. 2010.

[13] C. H. Chang and K. L. Wong, "Small-size printed monopole with a printed distributed inductor for penta-band WWAN mobile phone application," *Microwave Opt. Technol. Lett.*, vol. 51, pp. 2903–2908, Dec. 2009.

[14] K. L. Wong and T. W. Kang, "GSM850/900/1800/1900/UMTS printed monopole antenna for mobile phone application," *Microwave Opt. Technol. Lett.*, vol. 50, pp. 3192–3198, Dec. 2008.

[15] , S. Sesia, I. Toufik, and M. Baker, Eds., *LTE, The UMTS Long Term Evolution: From Theory to Practice*. New York: Wiley, 2009.
[16] J. Cho and K. Kim, "A frequency-reconfigurable multi-port antenna operating over LTE, GSM, DCS, and PCS bands," presented at the IEEE Antennas Propag. Soc. Int. Symp., Charleston, SC, 2009, Session 317.
[17] G. Park, M. Kim, T. Yang, J. Byun, and A. S. Kim, "The compact quad-band mobile handset antenna for the LTE700 MIMO application," presented at the IEEE Antennas Propag. Soc. Int. Symp., Charleston, SC, 2009, Session 307.
[18] K. L. Wong, L. C. Chou, and C. M. Su, "Dual-band flat-plate antenna with a shorted parasitic element for laptop applications," *IEEE Trans. Antennas Propag.*, vol. 53, pp. 539–544, Jan. 2005.
[19] M. Ozkar, "Multi-band bent monopole antenna," U.S. patent 7,405,701 B2, Jul. 29, 2008.
[20] Y. X. Guo, M. Y. W. Chia, and Z. N. Chen, "Miniature built-in quad-band antennas for mobile handsets," *IEEE Antennas Wireless Propag. Lett.*, vol. 2, pp. 30–32, 2003.
[21] A. Lehtola, "Internal Multi-band antenna," U.S. patent 6,476,769 B1, Nov. 5, 2002.
[22] Ansoft Corporation HFSS [Online]. Available: http://www.ansoft.com/products/hf/hfss/
[23] K. L. Wong, *Planar Antennas for Wireless Communications*. New York: Wiley, 2003.
[24] T. Y. Wu and K. L. Wong, "On the impedance bandwidth of a planar inverted-F antenna for mobile handsets," *Microwave Opt. Technol. Lett.*, vol. 32, pp. 249–251, Feb. 2002.
[25] P. Vainikainen, J. Ollikainen, O. Kivekas, and I. Kelander, "Resonator-based analysis of the combination of mobile handset antenna and chassis," *IEEE Trans. Antennas Propag.*, vol. 50, pp. 1433–1444, Oct. 2002.
[26] *Safety Levels With Respect to Human Exposure to Radio-frequency Electromagnetic Field, 3 kHz to 300 GHz*, ANSI/IEEE standard C95.1, Apr. 1999.
[27] SEMCAD Schmid & Partner Engineering AG (SPEAG) [Online]. Available: http://www.semcad.com
[28] C. H. Li, E. Ofli, N. Chavannes, and N. Kuster, "Effects of hand phantom on mobile phone antenna performance," *IEEE Trans. Antennas Propag.*, vol. 57, pp. 2763–2770, Sep. 2009.
[29] C. T. Lee and K. L. Wong, "Internal WWAN clamshell mobile phone antenna using a current trap for reduced groundplane effects," *IEEE Trans. Antennas Propag.*, vol. 57, pp. 3303–3308, Oct. 2009.

Bandwidth Enhancement of the Small-Size Internal Laptop Computer Antenna Using a Parasitic Open Slot for Penta-Band WWAN Operation

Kin-Lu Wong, Wei-Ji Chen, Liang-Che Chou, and Ming-Ren Hsu

***Abstract*—By embedding a parasitic open slot in the antenna ground of a small-size internal laptop computer antenna, enhanced bandwidth for the antenna's lower band to cover the GSM850/900 operation (824–960 MHz) can be achieved. The internal laptop computer antenna in this study is a small-size coupled-fed shorted T-monopole, whose length along the top edge of the display ground of the laptop computer is 43 mm only. The antenna can also provide a wide upper band to cover the GSM1800/1900/UMTS operation (1710–2170 MHz). With the inclusion of the parasitic open slot, the total antenna length along the top edge of the display ground is 48 mm only, and the occupied antenna volume is $10 \times 3.5 \times 48$ mm^3 above the top edge of the display ground, which is the smallest for the internal penta-band WWAN laptop computer antenna that have been reported for the present. Detailed results of the proposed parasitic open slot on bandwidth enhancement of the internal WWAN laptop computer antenna are presented.**

***Index Terms*—Bandwidth enhancement, laptop computer antennas, mobile antennas, open slot, WWAN antennas.**

I. Introduction

In order to provide ubiquitous wireless internet access, the internal antennas for wireless wide area network (WWAN) communications have been demanded in the modern laptop computers. It is required that the internal WWAN laptop computer antennas be with smaller size yet wider bandwidth to cover the penta-band operation of the GSM850 (824–894 MHz),GSM900 (880–960 MHz), GSM1800 (1710–1880 MHz), GSM1900 (1850–1990 MHz) and UMTS (1920–2170 MHz) systems. For the internal WWAN laptop computer antennas that have recently been reported [1]–[7], however, it is required that the length of the antenna along the top edge of the display ground should be at least 60 mm for penta-band WWAN operation. This length requirement is needed for these reported internal antennas to generate the desired operating band at about 900 MHz to cover the GSM850/900 operation. This behavior is owing to the much larger display ground connected to the internal WWAN antenna. The large display ground cannot assist in the generation of a wide lower band at about 900 MHz for the WWAN antenna. This behavior is different from the internal antennas connected to the system ground plane of the mobile phone, which has a much smaller size than the display ground and is generally excited as an efficient radiator in the 900-MHz band [8].

In this communication we present a new bandwidth-enhancement method of using a parasitic open slot to achieve a wide lower band for the internal laptop computer antenna with a small size (antenna length less than 50 mm along the top edge of the display ground) to

Manuscript received December 11, 2009; revised February 25, 2010; accepted March 25, 2010. Date of publication July 01, 2010; date of current version October 06, 2010.

K.-L. Wong and W.-J. Chen are with the Department of Electrical Engineering, National Sun Yat-sen University, Kaohsiung 80424, Taiwan (e-mail: wongkl@ema.ee.nsysu.edu.tw; wongkl@mail.nsysu.edu.tw; chenwj@ema.ee.nsysu.edu.tw).

L.-C. Chou and M.-R. Hsu are with the Department of High Frequency Business, Yageo Corporation Nantze Branch, Kaohsiung 811, Taiwan (e-mail: vincent.chou@yageo.com; hsumr@yageo.com).

Color versions of one or more of the figures in this communication are available online at http://ieeexplore.ieee.org.

Digital Object Identifier 10.1109/TAP.2010.2055815

射 频 和 天 线 设 计 培 训 课 程 推 荐

易迪拓培训(www.edatop.com)由数名来自于研发第一线的资深工程师发起成立，致力并专注于微波、射频、天线设计研发人才的培养；我们于 2006 年整合合并微波 EDA 网(www.mweda.com)，现已发展成为国内最大的微波射频和天线设计人才培养基地，成功推出多套微波射频以及天线设计经典培训课程和 ADS、HFSS 等专业软件使用培训课程，广受客户好评；并先后与人民邮电出版社、电子工业出版社合作出版了多本专业图书，帮助数万名工程师提升了专业技术能力。客户遍布中兴通讯、研通高频、埃威航电、国人通信等多家国内知名公司，以及台湾工业技术研究院、永业科技、全一电子等多家台湾地区企业。

易迪拓培训课程列表：http://www.edatop.com/peixun/rfe/129.html

射频工程师养成培训课程套装

该套装精选了射频专业基础培训课程、射频仿真设计培训课程和射频电路测量培训课程三个类别共 30 门视频培训课程和 3 本图书教材；旨在引领学员全面学习一个射频工程师需要熟悉、理解和掌握的专业知识和研发设计能力。通过套装的学习，能够让学员完全达到和胜任一个合格的射频工程师的要求…

课程网址：http://www.edatop.com/peixun/rfe/110.html

ADS 学习培训课程套装

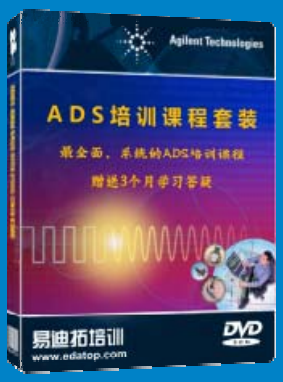

该套装是迄今国内最全面、最权威的 ADS 培训教程，共包含 10 门 ADS 学习培训课程。课程是由具有多年 ADS 使用经验的微波射频与通信系统设计领域资深专家讲解，并多结合设计实例，由浅入深、详细而又全面地讲解了 ADS 在微波射频电路设计、通信系统设计和电磁仿真设计方面的内容。能让您在最短的时间内学会使用 ADS，迅速提升个人技术能力，把 ADS 真正应用到实际研发工作中去，成为 ADS 设计专家...

课程网址： http://www.edatop.com/peixun/ads/13.html

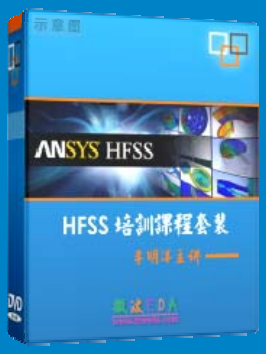

HFSS 学习培训课程套装

该套课程套装包含了本站全部 HFSS 培训课程，是迄今国内最全面、最专业的 HFSS 培训教程套装，可以帮助您从零开始，全面深入学习 HFSS 的各项功能和在多个方面的工程应用。购买套装，更可超值赠送 3 个月免费学习答疑，随时解答您学习过程中遇到的棘手问题，让您的 HFSS 学习更加轻松顺畅…

课程网址：http://www.edatop.com/peixun/hfss/11.html

CST 学习培训课程套装

该培训套装由易迪拓培训联合微波 EDA 网共同推出，是最全面、系统、专业的 CST 微波工作室培训课程套装，所有课程都由经验丰富的专家授课，视频教学，可以帮助您从零开始，全面系统地学习 CST 微波工作的各项功能及其在微波射频、天线设计等领域的设计应用。且购买该套装，还可超值赠送 3 个月免费学习答疑…

课程网址：http://www.edatop.com/peixun/cst/24.html

HFSS 天线设计培训课程套装

套装包含 6 门视频课程和 1 本图书，课程从基础讲起，内容由浅入深，理论介绍和实际操作讲解相结合，全面系统的讲解了 HFSS 天线设计的全过程。是国内最全面、最专业的 HFSS 天线设计课程，可以帮助您快速学习掌握如何使用 HFSS 设计天线，让天线设计不再难…

课程网址：http://www.edatop.com/peixun/hfss/122.html

13.56MHz NFC/RFID 线圈天线设计培训课程套装

套装包含 4 门视频培训课程，培训将 13.56MHz 线圈天线设计原理和仿真设计实践相结合，全面系统地讲解了 13.56MHz 线圈天线的工作原理、设计方法、设计考量以及使用 HFSS 和 CST 仿真分析线圈天线的具体操作，同时还介绍了 13.56MHz 线圈天线匹配电路的设计和调试。通过该套课程的学习，可以帮助您快速学习掌握 13.56MHz 线圈天线及其匹配电路的原理、设计和调试…

详情浏览：http://www.edatop.com/peixun/antenna/116.html

我们的课程优势：

※ 成立于 2004 年，10 多年丰富的行业经验，

※ 一直致力并专注于微波射频和天线设计工程师的培养，更了解该行业对人才的要求

※ 经验丰富的一线资深工程师讲授，结合实际工程案例，直观、实用、易学

联系我们：

※ 易迪拓培训官网：http://www.edatop.com

※ 微波 EDA 网：http://www.mweda.com

※ 官方淘宝店：http://shop36920890.taobao.com